**Original Article**

e-ISSN: 2581-0545 - https://journal.itera.ac.id/index.php/jsat/

# Semi-Empirical Estimation of Velocity Profile for Shallow Gravel Bed Channel

Received 7 February 2022
Accepted 2 August 2022
Published 30 December 2022

Open Access

DOI: 10.35472/jsat.v6i2.885

Rahma Yanda [*a], Morihiro Harada [b], Ichiro Tamagawa [b]

[a] *Program Studi Rekayasa Tata Kelola Air Terpadu, Institut Teknologi Sumatera*

[b] *River Basin Research Center, Gifu University*

** Corresponding E-mail: rahma.yanda@tka.itera.ac.id*

**Abstract**: The dependence of flow velocity distribution near the bed on the roughness geometry has led to various approaches for estimating the velocity. The models proposed by previous studies are mostly based on segmented velocity profiles (e.g., a linear distribution within the interfacial sublayer and logarithmic distributions above the interfacial sublayer). By increasing number of segments, the possibility of errors in the parameters, as well as constants, are likely to rise. This study assessed the applicability of a hyperbolic tangent function velocity model to estimate double-averaged velocity profile for shallow flow over a rough gravel bed as a single model concept, especially for the area within roughness layer. Velocity profiles over gravel beds with different arrangements and roughness densities from previously published studies using laboratory measurements were used to validate this model. The behaviours of related constants for this model in response to changes in the flow depth and roughness geometry were investigated, and limitations on it application were evaluated. It was found that the constants required to apply hyperbolic tangent function are affected by roughness geometry function and relative submergence. Through this study also observed that HTF is reliable to describe the velocity profile for about twice of geometric roughness height.

**Keywords:** *velocity profile, roughness layer, gravel bed, roughness geometry function, hyperbolic tangent function*

## Introduction

The hydrodynamics of flow near the bed of gravel bed streams have been the focus of numerous studies for decades because the flow velocity distribution highly depends on the roughness geometry of the gravel bed [1], which is known to be highly heterogeneous. Meanwhile, information about velocity profile is one of important factor used to understand hydrodynamics of flow, calculate sediment transport, and to evaluate river habitat conditions.

Area where the flow is strongly affected by the heterogeneity of roughness geometry is known as roughness layer [2, 3]. Conditions with heterogeneous roughness causes velocity profile, which is often obtained through logarithmic law and only based on one point measurement, to deviate [4-6]. Therefore, double-averaging method (or DAM), where time and space velocity are considered (detail in [7]) has been widely applied to link the relationship between heterogeneity of local flow properties, such as velocity, with spatial bed conditions or bed roughness. In that way, velocity profiles can be able to show more representative distribution of spatial bed conditions.

Several studies had reported that the double-averaged velocity distribution within roughness layer also showed a deviation from logarithmic law (or log law), which is a typical velocity distribution in streams with a smooth bed or when flow depth $H$ to the degree of bed roughness, characterized by the representative grain size diameter $D$, ratio is high or also known as high relative submergence [5, 6]. However, other studies found that the logarithmic law is still applicable to describe the velocity distribution in the area above the roughness layer [2, 4, 8].

Meanwhile, for shallow flows, where the relative submergence is less than 4 (i.e., $H/D \leq 4$ [9]), bed roughness may affect the whole depth velocity distribution [10]. Various efforts have been made to understand the relations among flows, roughness geometry changes, and velocity distributions. For example, Nikora *et al*. [1] proposed some velocity distribution models (i.e., constant velocity, exponential, and linear distribution models) that possibly exist within the area between the roughness trough $z_t$ and

the roughness crest $z_c$ (i.e., the interfacial sublayer). This layer is identified as a part of the roughness layer [11]. Although that study suggested that a linear velocity model might be applicable to flows with wide ranges of relative submergence and roughness types, the possibility of these models to exist as single model or as a combination (i.e., linear-log or linear-exponential profiles) which depends on flow condition and roughness geometry on flow was noticed. However, further investigation about it had not been done because of the limited detailed information about the roughness geometry (e.g., the roughness geometry function $\varphi$ ($z$)) in their data set.

In a study conducted by Nikora *et al* [1], the combination of linear and logarithmic velocity models was tested on time-averaged velocity profiles. As one of important parameters to be considered in logarithmic velocity equation, universal von Kármán constant with value of $\kappa$ = 0.4 was used. The results found that this combination can approximately describe the measured time-averaged velocity for the area within and above the interfacial sublayer, respectively. Nevertheless, various studies had reported that the logarithmic law applied in shallow flow and rough bed conditions has values that differ from $\kappa$ = 0.4 and depends on the roughness height and relative submergence [10, 12]. Furthermore, several other problems related to the parameterization of the logarithmic law in shallow flows have also been observed. For example, it is difficult to determine the definition of the geometric roughness height and the upper boundary of the roughness layer (e.g., [13, 14]) and to define the height origin of the logarithmic distribution (the so-called zero-plane displacement $z_{dp}$) [15]. Each study also noted that the observed problems might be related to the roughness geometry. However, the roughness geometry data (e.g., $\varphi$ ($z$)) were mostly unavailable or under investigation in these mentioned papers. Moreover, estimating velocity profiles for shallow flows using a combination velocity profile approach may lead to some errors caused by the uncertainties in the parameterization. Thus, these issues require further investigations and also suggest that further development of another approach may be appropriate.

In another study conducted by Katul *et al* [16] proposed the hyperbolic tangent function (HTF), which is based on a mixing layer analogy where faster-moving fluids above the bed roughness area and slower-moving fluids within the bed roughness (i.e., interfacial sublayer). These two areas are connected at what is known as an inflection point and create an S-shaped velocity profile. This S-shaped velocity profile has commonly been observed in velocity measurements conducted under shallow flow conditions in gravel bed streams (e.g., [17]-[19]).

Although the potential of HTF to describe the velocity of shallow flows has been widely discussed (e.g., [1], [20], [21]) and HTF-based bulk velocity estimations have shown good consistency with calculations of many data sets [14], It was observed that the capability of this model to describe a double-averaged velocity profile with various roughness geometry conditions remains less examined than that of other models (i.e., the linear and logarithmic distribution model). Thus, more detailed investigation is needed in the case of describing velocity profiles by using HTF in shallow conditions.

Based on some challenges related to parameterization of velocity distribution (von Kármán constant $\kappa$, roughness geometry, relative submergence) and velocity distribution models to determine suitable velocity distributions for shallow flow, in this study, a semi-empirical approach to estimate a two-dimensional (2D) velocity profile for shallow flow over rough gravel beds was tested. The applicability of HTF as one of potential models was chosen and examined.

This approach was started by calculating bulk flow properties (i.e., bulk velocity, shear velocity, and flow depth) from data sets specially choose for this study using combinations of flow resistance equation proposed by Ferguson [22] and dimensionless hydraulic geometry equations. These combinations, which is known as Variable Power Equation (VPE), had been applied to 2980 data set of field measurements with variability of relative submergence in a study conducted by Rickenmann and Recking [23] and it showed a better results compared to other well-known flow resistance equations. Then, bulk flow properties later were used as inputs in HTF. Predicted and measured velocity profiles were compared in order to know the capability of this semi-empirical approach.

In order to minimize the source of errors due to the uncertainties of parameterization, in this study, HTF was assumed to be able to describe the whole depth velocity profile (i.e., from roughness trough to water surface) for a given data set with a relative submergence range from 2 to 4. To apply the HTF model, two unknown constants, $C_u$ and $\alpha$, are required. To determine the value of $C_u$ and $\alpha$ which is considering relative submergence, as well as various roughness densities, arrangements, and roughness geometry function. The approach with a published laboratory data set was also validated in this study. A comparison between the constant values obtained via our new approach and the original values from [14] was


*Published by: Lembaga Penelitian dan Pengabdian Masyarakat (LPPM)*
*Institut Teknologi Sumatera, Lampung Selatan, Indonesia*

performed. As a reference, a comparison between the velocity profiles estimated using the HTF model (i.e., the single model concept) and a combination of linear and logarithmic distribution models is also presented.

First, brief explanations of the flow resistance of the VPE and the HTF velocity distribution model are provided in the Methods and Materials section. Next, the details of our proposed semi-empirical approach for estimating the velocity profile and for determining the constants used in the HTF are described. Then, data sets compiled from previously published studies that contain double-averaged velocity profiles from measurements are used for validation, and the results are shown. Finally, the applicability of this approach and its limitations are discussed, and conclusions are provided.

## Method and Materials

### Variable Power Equation (VPE)

Rickenmann and Recking [23] combined the flow resistance equation proposed by Ferguson [22] (Eq. 1), with dimensionless hydraulic geometry equations (Eq. 2 and 3). The final form is written as Eq. 4.

$$U/u_* = a_1 a_2 (H/D_{84}) / \left\{ a_1^2 + a_2^2 (H/D_{84})^{5/3} \right\}^{1/2} \quad \textbf{(1)}$$

$$q^{**} = q/\sqrt{gSD_{84}^3} \quad \textbf{(2)}$$

$$U^{**} = U/\sqrt{gSD_{84}} \quad \textbf{(3)}$$

$$a_1^2 U^{**^5} + a_2^2 U^{**^{10/3}} q^{**^{5/3}} = a_1^2 a_2^2 q^{**^3} \quad \textbf{(4)}$$

with $a_1$ = 6.5 and $a_2$ = 2.5, as suggested in [22]. $U$ is depth-averaged velocity; $u_*$ is shear velocity; $H$ is flow depth; $D84$ is diameter of bed material corresponds to 84% of the sampled area; $q$ is unit discharge; $S$ is bed or energy slope; $g$ is gravity. This combination has been confirmed to provide better results for predicting bulk flow velocity than the Manning-Strickler and Keulegan equations, especially under intermediate relative submergence conditions [23]. The good performance shown by VPE is due to the consideration of two different velocity profiles that commonly exist in shallow rough streams: a linear profile within the roughness layer and a logarithmic profile above it (e.g., [1], [12]). Additionally, with this combination, one of the sources of errors that comes from inaccurate flow depth measurements due to irregular bed topography may be reduced.

### Hyperbolic Tangent Function (HTF)

The process of momentum transfer in the mixing layer analogy is induced by vorticity through Kelvin-Helmholtz instabilities and is described by the HTF, as shown in equation (5). The HTF contains two constants: 1) a constant that describes the ability of a fluid to penetrate into roughness element, $\alpha$, and 2) a constant that expresses flow resistance at the interface between fast- and slow-moving fluids, $C_u$.

$$\frac{U}{u_i} = \frac{1}{H}\int_0^H \left[1 + tanh\left(\frac{z-D}{\alpha D}\right)\right] dz = 1 + \frac{\alpha D}{H} ln\left(\frac{cosh\left(\frac{1}{\alpha} - \frac{H}{\alpha D}\right)}{cosh\left(\frac{1}{\alpha}\right)}\right) \quad \textbf{(5)}$$

The term $\alpha D$ is comparable to the length shear scale $L_s$, which is typically produced by a Kelvin-Helmholtz type instability at $z = D$, where $u_i$ is the mean reference velocity at $z = D$ [24], [25] and is described as $u_i = C_u u_*$. With the integration of Eq. 5 and a transformation of Eq. 6, flow resistance can be calculated (Eq. 7), where $\xi = H/D$, shear velocity $u_*=\sqrt{gHS}$, $g$ is the gravitational force and $S$ is the bed or energy slope.

$$\mathrm{f}(\xi, \alpha) = 1 + \alpha \frac{1}{\xi} ln\left(\frac{cosh\left(\frac{1}{\alpha} - \frac{1}{\alpha}\xi\right)}{cosh\left(\frac{1}{\alpha}\right)}\right) \quad \textbf{(6)}$$

$$U/u_* = C_u f(\xi.\alpha) \quad \textbf{(7)}$$

Katul *et al*. [16] noted that the result of Eq. 7 is highly dependent on the definition of $D$ and then used $D \sim D_{84}$ because this value is common for natural gravel bed streams.

In their study, Katul *et al*. [16] chose $C_u \approx 4.5$ and $\alpha = 1$ for use in the HTF for gravel bed streams. $C_u \approx 4.5$ was obtained by averaging $C_u$ calculated from dense canopies ($C_u \approx 3.3$) [25], [26] and rough-wall boundary layers ($C_u \approx 5.8$), which was calculated based on the log law using Eq. 8,

$$C_u \approx 1/\kappa \ln(D_{84}/z_0) \quad \textbf{(8)}$$

by assuming $z_o \sim D_{84}/10$ [27], [28], where $z_o$ is the zero-plane displacement. Meanwhile, $\alpha = 1$ was applied with the expectation that the sizes of the instabilities defining $L_s$ are as large as the obstacle size $D_{84}$. This condition was illustrated through roughness concentration from gravel bed streams, demonstrating that the roughness concentration was distributed within the lower 20% of $D_{84}$ for the gravel bed stream.

To show the effect of each constant on the velocity profile, this study presents a simple description in Figure 1. The velocity profile calculated using the HTF with $\alpha = 1$ exhibits a modest inflection point, which appears similar to the combination of the linear and logarithmic profiles in [10]. The application of $\alpha = 1$ shows the condition in which the fluid can penetrate deeper into the bed roughness and also implies that the bed roughness produces a higher resistance

to the flow which causes a slower velocity than that of $\alpha$ = 0.5 for $z/D > 1$. Theoretically, the mixing length $L_M$ of the mixing layer is twice that of $L_s$ (i.e., $L_m = 2L_s$) [29], and the effect of deeper penetration may extend farther above the bed depending on the bed roughness. For example, if bed roughness is represented by $D_{84}$, then the bed roughness will affect the flow for approximately $L_M = 2L_s \approx 2\alpha D_{84}$. Meanwhile, the constant $C_u$ is affected by $u_*$, which increases as the shear decreases. In other words, $\alpha$ and $C_u$ are the dominant factors in the vertical and horizontal directions, respectively.

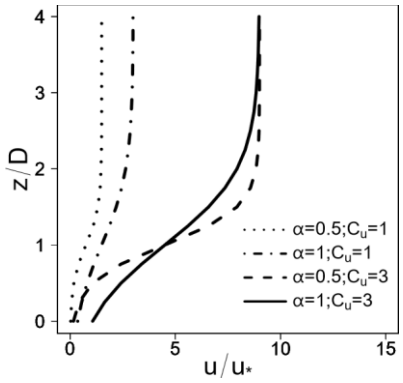


**Figure 1**. Description of the behaviors of constants (i.e., $\alpha$ and $C_u$) in the HTF.

### Approach for Velocity Profile Estimation

For shallow flows (i.e., $H/\delta \leq 4$), it was assumed that the flow resembles a mixing layer analogy, so the HTF is expected to be able to describe the double-averaged velocity profile of the whole depth. To apply HTF, the two constants in the equation (i.e., $C_u$ and $\alpha$) need to be determined. First, instead of calculating $C_u$ by using Eq. 8 which assumes the existence of logarithmic velocity within the roughness layer, this study propose another method. Considering its better performance in estimating flow resistance, the VPE was used to calculate $C_u$. The scheme of the approach in this study is illustrated in Figure 2. From several parameters, such as $D$, $B$, $S$ and $Q$, unit discharge $q$ can be calculated by $q = Q/B$, which is then used to obtain $q^{**}$ in Eq. 2. Furthermore, through the iterative process, $U^{**}$ can be calculated using Eq. 4 and is then used to calculate bulk velocity $U_{b\ calc}$. In this study, because the representative grain size diameter $D$ in the data sets was not available for all cases, instead of applying $D \sim D_{84}$, the geometric roughness height $\delta$ was employed, where $\delta = z_c - z_t$.

Next, information on the flow depth can be obtained using $H_{calc} = Q/BU_{b\ calc}$, which is then used to calculate shear velocity $u_*$. Pokrajac *et al*. [30] suggested using shear velocity at the crest $u_{*c}$ for streams in which the bed roughness is comparable to the flow depth,

$$u_{*calc} = \sqrt{g(H_{calc} - \delta)S} \quad \textbf{(9)}$$

because it is a more appropriate velocity scale for scaling turbulent flow quantities across the whole flow profile. Then, after $U_{b\ calc}$ and $u_{*c\ calc}$ are obtained, $U_{b\ calc}/u_{*c\ calc}$ is inserted into Eq. 7,

$$U_{b\ calc}/u_{*c} = C_u f \quad \textbf{(10)}$$

$C_u$ can be calculated and is written as $C_{u\ VPE}$.

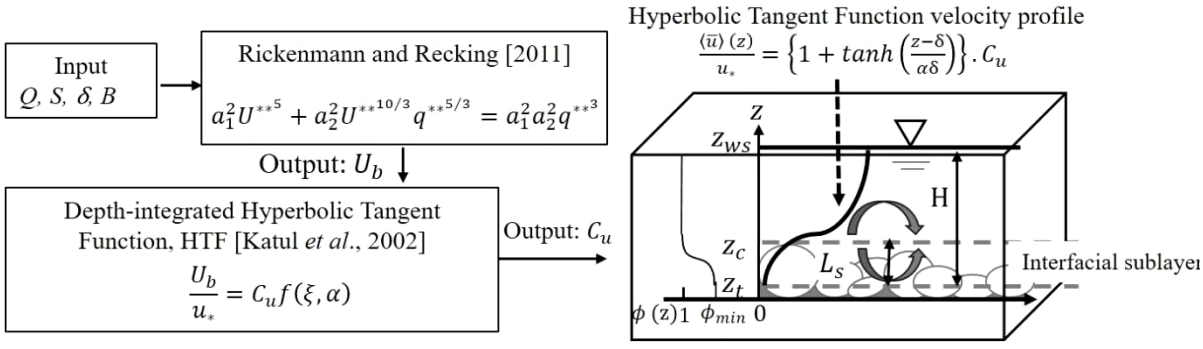


**Figure 2**. Scheme to estimate double-averaged velocity profile. $Q$ is discharge, $H$ is flow depth, $S$ is bed or energy slope, δ is geometric roughness height, $B$ is stream width, $U_b$ is bulk velocity, $u_*$ is shear velocity, $\phi$ is porosity, $L_s$ is length shear scale, $z_{ws}$ is water surface elevation, and $z_c$ and $z_t$ are the bed roughness crest and trough, respectively.


*Published by: Lembaga Penelitian dan Pengabdian Masyarakat (LPPM)*
*Institut Teknologi Sumatera, Lampung Selatan, Indonesia*

**Table 1.** Summary of Hydraulic Conditions.

| Reference | Code | $Q$ (m³/s) | $B$ (m) | $\delta$ (m) | $H/\delta$ | $S$ |
|---|---|---|---|---|---|---|
| Ferreira (2008) | A1 | 0.023 | 0.4 | 0.054 | 2.85 | 0.004 |
| | A2 | 0.023 | 0.4 | 0.051 | 2.92 | |
| | A3 | 0.023 | 0.4 | 0.039 | 3.26 | |
| Habib *et al*. (2016) | B1 | 0.020 | 0.5 | 0.040 | 3.00 | 0.001 |
| | B2 | 0.024 | 0.5 | 0.030 | 4.00 | |
| Yanda *et al*. (2016) | C1 | 0.065 | 0.5 | 0.144 | 2.02 | 0.009 |
| | C2 | 0.080 | 0.5 | 0.120 | 2.35 | |
| | C3 | 0.078 | 0.5 | 0.093 | 2.56 | |

a) Bed condition of A1 [31]

b) Bed conditions of B1 and B2 [32]

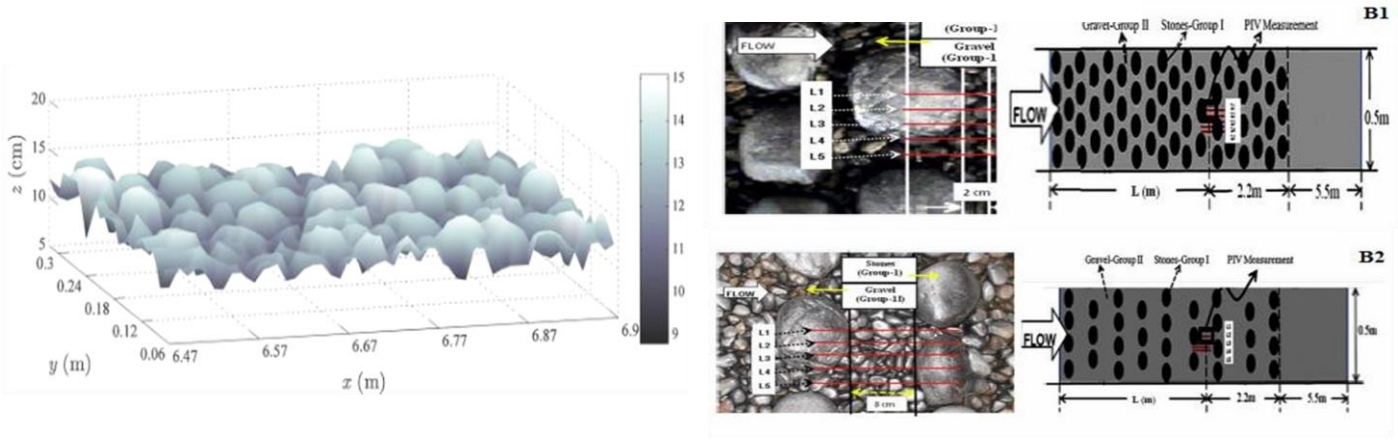


c) Bed conditions of C1, C2 and C3 [33]

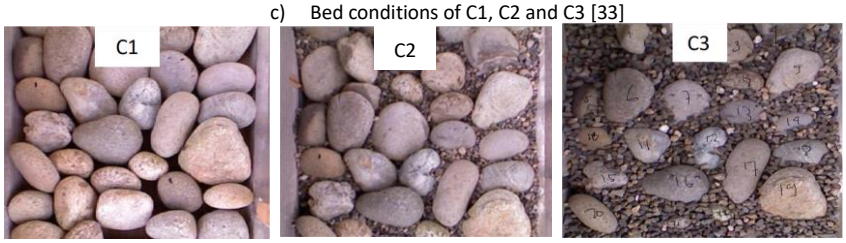


**Figure 3**. Immobile bed conditions with different arrangements and roughness densities.

Meanwhile, for $\alpha$, it was assumed that bed conditions of our data sets might be different from those used in [16] as a reference. Thus, as a first approximation, $\alpha$ was obtained by fitting the double-averaged velocity from the measurement below the inflection point using the HTF equation for the velocity profile.

$$\frac{\langle\overline{u}\rangle(z)}{\langle\overline{u}\rangle_i} = \left(1 + \tanh\left(\frac{z-\delta}{\alpha\delta}\right)\right) \qquad \textbf{(11)}$$

The inflection point was assumed to be at the bed roughness crest $z_c$, so $\langle\overline{u}\rangle_i \sim \langle\overline{u}\rangle_{z_c}$ is applied in Eq. 11 and is written as $\alpha_{fit}$. For comparison to $C_{u\ VPE}$, $C_u$ obtained by fitting the measured velocity profiles using Eq. 11 is also presented.

**Data Sets**

To test this approach, a range of laboratory data (Table 1) that included gravel beds with different arrangements and roughness densities were collected. The relative submergence ranged from 2 to 4 ($2 \leq H/\delta \leq 4$). For A1, the

**Table 2.** Depth-Averaged Roughness Geometry Function $\varphi_m$ and Porosity $\phi$.

| | A1 | A2 | A3 | C1 | C2 | C3 |
|---|---|---|---|---|---|---|
| $\varphi_m$ | 0.65 | 0.66 | 0.72 | 0.39 | 0.43 | 0.53 |
| $\phi$ | 0.38 | 0.31 | 0.22 | 0.35 | 0.29 | 0.31 |

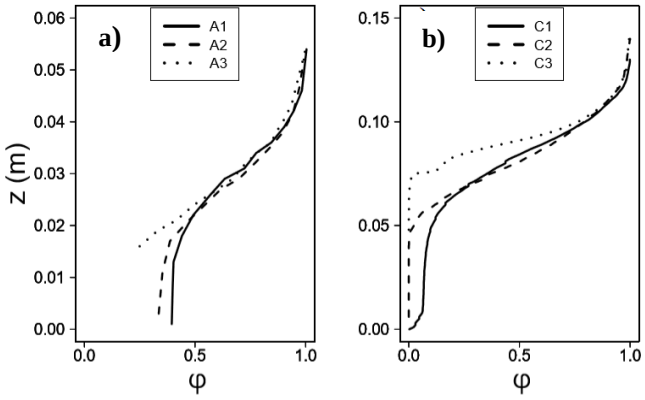


**Figure 4.** a) Roughness geometry profiles $\varphi$ (z) A1-A3 from [27]; b) Roughness geometry function profiles $\varphi$ (z) for C1-C3 from [29]

bed consisted of an openwork gravel bed (i.e., a gravel bed without sand) with randomly arranged clasts; the interclast space in this bed was then filled with sand in A2. A higher sand content was used in A3. Meanwhile, for B1 and B2 [31], cobbles were arranged in staggered-packed and staggered-loose arrangements, respectively. In B1, cobbles were placed directly on the gravel layer, while in B2, cobbles were buried 1 cm into the gravel layer to create different relative submergences [32]. Furthermore, in C1, the bed consisted of an openwork cobble bed arranged to imitate imbrication (i.e., upstream particles overlap the downstream particles), and the interclast space was then filled with gravels in C2. Additionally, the gravel content was increased in C3 [33]. The figures of each bed condition are shown in Figure 3. Bed forms of A2 and A3 were not shown in study conducted in [31], but the information related to roughness geometry is exist. All the beds in these data sets were immobile except for A3, which was subjected to equilibrium sediment transport conditions. However, bed-forms were avoided, so A3 was comparable to A1 and A2. For A1-A3 and C1-C3, information on the roughness geometry function $\varphi$ (z), which defines the ratio of volume occupied only by fluid to the total volume of solids from $z_c$ to $z_t$, the depth-averaged roughness geometry function $\varphi_m$ and the bulk porosity $\phi$ was also obtained (Table 2 and Figure 4).

The double-averaged velocity profiles for each case in Table 1 normalized by velocity measurements at the crest $\langle\overline{u}\rangle_c$ are shown in Figure 5. The minimum bed elevation (or roughness trough $z_t$) in the experiment was set as the origin of the vertical coordinate for the velocity profiles following [5]. The profiles seemed quite similar to the S-shaped pattern of the mixing layer in canopy flows (i.e., [16], [25]) with noticeable modest inflection points.

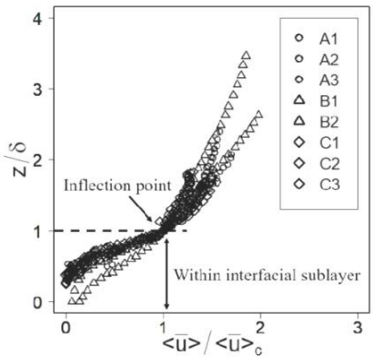


**Figure 5.** Normalized double-averaged velocity profiles from the data sets.

## Results And Discussion

### Determination of Constants for Hyperbolic Tangent Function

To confirm the performance of VPE to calculate $U_b$ for our data sets, its comparison with other well-known flow


*Published by: Lembaga Penelitian dan Pengabdian Masyarakat (LPPM)*
*Institut Teknologi Sumatera, Lampung Selatan, Indonesia*

resistance equations was shown in Figure 6, such as;

Manning-Strickler [34].

$$U/u_* = 8.3\ (h/D_{90})^{1/6} \quad \textbf{(12)}$$

and Hey [1979].

$$U/u_* = 6.25 + 5.75\log(h/3.5D_{84}) \quad \textbf{(13)}$$

This result confirmed the investigation performed by Rickenmann and Recking [23], where VPE showed better performance compared to the Manning-Strickler and Hey equations.

Value of $\alpha$ as one of constant in HTF model (Eq.5) obtained by fitting (i.e., $\alpha_{fit}$) using velocity profiles from measurement below the inflection point which the detail can be seen in Figure 7a. The results from fitting is plotted against relative submergence as can be seen in Figure 7b. The $\alpha_{fit}$ from data set was found to vary from 0.4 to 1. Similar values of $\alpha$ were obtained in another studies, where α approximately 0.5 has been found for vegetation canopies (e.g., [25], [26]) while $\alpha$ = 1 for gravel streams (e.g., [16]). The $\alpha_{fit}$ values implies that for A1-A3, B1, and C1-C3 might had similar roughness characteristics with vegetation canopies which is relatively dense compared to B2. In B2, roughness geometry is relatively sparse so that the flow can penetrate more into roughness element.

The roughness geometry function changes if the roughness element density changes, which affects the flow below the roughness crest. Figure 7b presents the effect of $\varphi_m$ on $\alpha_{fit}$, and it was found that as the bed arrangement became denser, $\varphi_m$ and the value of $\alpha_{fit}$ also decreased (i.e., $\varphi_m$ B2 > $\varphi_m$ A1 > $\varphi_m$ C1). Note that in Figure 7b, due to the unavailability of roughness geometry function information for B1 and B2, the determination of the roughness geometry function can only be estimated visually at this time. The difference of $\varphi_m$ of B1 was difficult to judge compared to

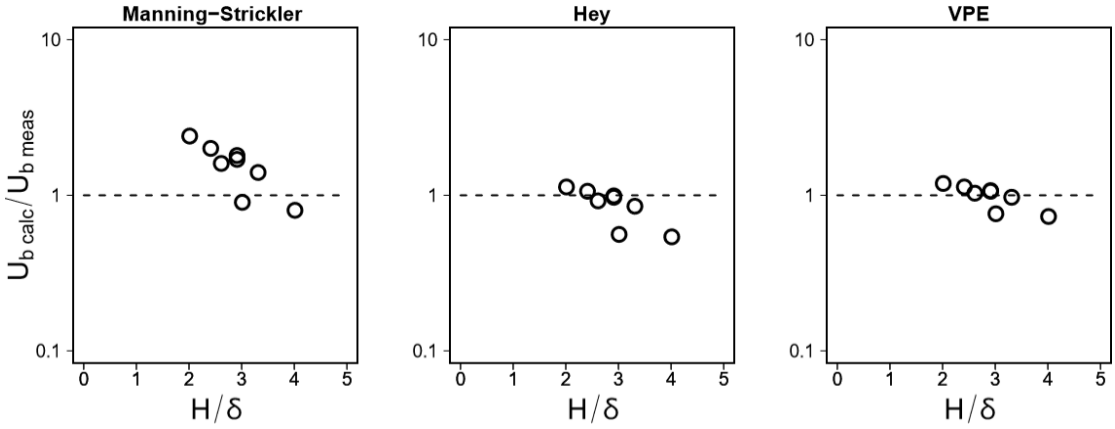


**Figure 6.** Comparisons of total depth bulk velocity values from measurements $U_{b\ meas}$ andcalculations $U_{b\,calc}$ using three flow resistance equations.

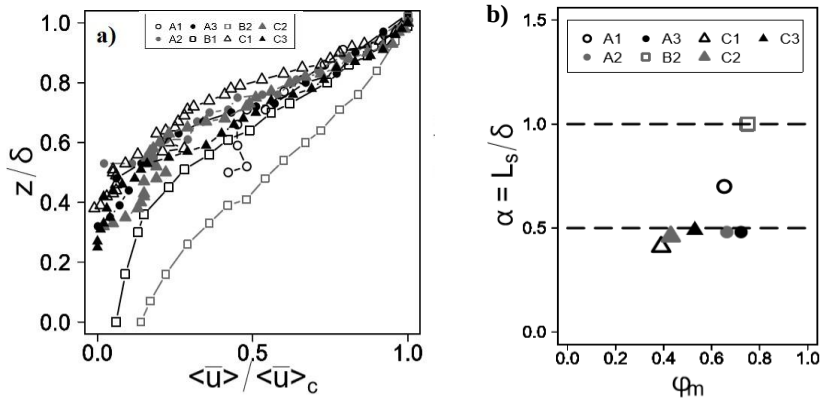


**Figure 7**. a) Normalized double- averaged velocity profiles within the interfacial sublayer; b) Relation of the $\alpha$ value obtained by fitting $\alpha_{fit}$ with the depth-aver roughness geometry function $\varphi_m$

A1, but B2 can obviously be expected to have a larger value of $\varphi_m$ among all cases. In contrast, the addition of finer sediment in C2, C3, A2 and A3 caused an increase in $\varphi_m$. Furthermore, this addition also increased $\alpha_{fit}$ for C2 and C3. Nevertheless, for A2 and A3, despite an increase in $\varphi_m$ and a decrease in δ, $\alpha_{fit}$ showed lower values compared to A1. This study argued that it might be caused by the different sizes of sediment mixtures. The details explanation for this condition is included in our discussion.

Further, $C_{u\ VPE}$ calculated by using Eq.10 was compared to $C_u$ fitted with Eq. 6 and 7. Characteristics of $C_u$ and the influence of relative submergence on values of $\alpha$ on $C_u$ were examined in Figure 8. The results showed two different patterns. First, $C_{u\ VPE}$ was found to increase significantly for cases with lower relative submergence (i.e., C1-C3) and decrease slightly or remain relatively constant when the relative submergence increases. Meanwhile, $C_{u\ fit}$ increased at first but then changed little as the relative submergence increased.

The effect of $\alpha$ = 0.5 and 1 seemed to be relatively insignificant on both $C_{u\ VPE}$ and $C_{u\ fit}$ (Figure 8). Averaged values of $C_{u\ VPE}$ for $\alpha$ = 1 and 0.5 were 5.13 and 5.02, respectively. These values are larger than the value of $C_u$ = 4.5 used in [1]. It is also smaller than the values of 5.8 for rough-wall boundary layers and 5.3 – 5.6 as suggested in [11] for natural and artificial gravel beds.

**Velocity Estimation**

Velocity profiles were estimated by using variations of $C_u$ and $\alpha$ and the results are shown in Figure 9. As reference, velocity profiles estimated by using a combination of linear and logarithmic velocity distribution or lin-log equations (Eq. 14 and 15) suggested by [11] were plotted.

Linear equation

$$\langle\bar{u}\rangle/u_* = C(z/\delta)\ for\ 0 \le Z \le \delta \quad \textbf{(14)}$$

Logarithmic equation

$$\langle\bar{u}\rangle/u_* = 1/\kappa \ln(Z/\delta) + C\ for\ (z_{ws} - z_t) \ge Z \ge \delta \quad \textbf{(15)}$$

where constant $C$, similar to $C_u$, is also dependent on the roughness geometry, where $C = \langle\bar{u}\rangle(\delta)/u_{*c}$. In previous study [11], value $C \approx 5.3 - 5.6$ was suggested for natural and artificial gravel beds. Thus, averaged value $C \approx 5.5$ were chosen to be applied in Eq. 14 and 15. Meanwhile, for von Karman constant $\kappa$, value $\kappa = 0.4$ was used.

The result showed that for area within interfacial sublayer, velocity profiles estimated using $\alpha$ = 1 clearly overestimated velocity profiles from measurements for the packed bed cases (i.e., B1 and C1) and beds with the addition of finer sediments (i.e., A2, A3, C2, and C3). Meanwhile, for relatively loose bed conditions (i.e., A1, B2), $\alpha$ = 1 showed a relatively better agreement. In other words,

**Table 3**. Discrepancy Ratio $A_r$ and Inter-Quartile Range (IQR) from the Estimated VelocityProfiles (See the Descriptions of A, B, C, D, and E in Figure 10).

**Depth-averaged velocity**

| | A | B | C | D | E |
|---|---|---|---|---|---|
| $A_r$ (%) | 6.6 ↓ | 8.9 ↓ | 17 ↓ | 3.8 ↓ | 15 ↓ |
| IQR | 0.38 | 0.33 | 0.24 | 0.062 | 0.31 |

**Interfacial Sublayer**

| | A | B | C | D | E |
|---|---|---|---|---|---|
| $A_r$ (%) | 16 ↑ | 21 ↓ | 3.0 ↑ | 14 ↓ | 22 ↑ |
| IQR | 0.61 | 0.38 | 0.38 | 0.12 | 0.69 |

**Above Interfacial Sublayer**

| | A | B | C | D | E |
|---|---|---|---|---|---|
| $A_r$ (%) | 9.5 ↓ | 2.5 ↓ | 19 ↓ | 0.50 ↑ | 23 ↓ |
| IQR | 0.27 | 0.33 | 0.19 | 0.060 | 0.21 |

↓: underprediction; ↑: overprediction. $A_r$ (%) = $[1 - (\langle U\rangle_{calc}/\langle U\rangle_{meas})_{\text{median}}]100\%$. IQR: 3rdquartile – 1st quartile.


*Published by: Lembaga Penelitian dan Pengabdian Masyarakat (LPPM)*
*Institut Teknologi Sumatera, Lampung Selatan, Indonesia*

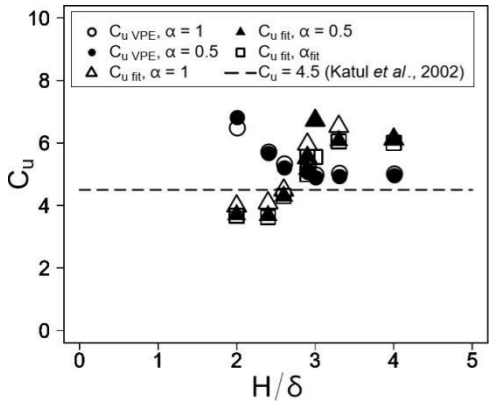


**Figure 8**. The effects of relative submergence $H/\delta$ on the value of $C_u$. $C_{u\ VPE}$ is calculated fromequation (10) with $\alpha$ = 1 and 0.5, $C_{u\ fit}$ is obtained by fitting the measured velocity profile to equation (11) using $\alpha$ equal to 0.5, 1 and $\alpha$fit

except for A1 and B2, $\alpha$ = 0.5 was suitable to use estimating velocity profiles within interfacial sublayer for all cases in these data sets.

Meanwhile for the area above the interfacial sublayer, even though previous result (Figure 8) showed insignificant effect of the value of $\alpha$ = 0.5 or 1 on $C_{u\ VPE}$, the estimated velocity profiles using $C_{u\ VPE}$ with $\alpha$ = 0.5 showed a better performance

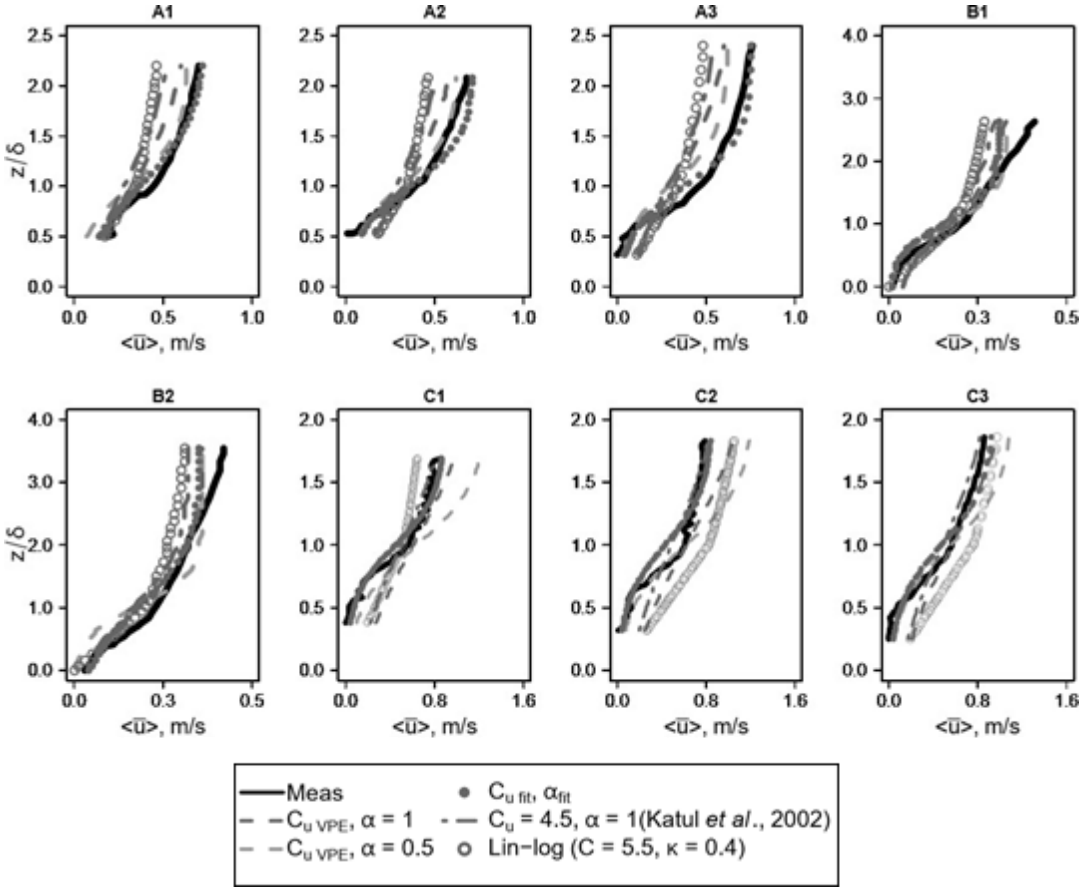


**Figure 9**. Comparison of velocity profiles velocity profiles calculated with HTF (Eq. 11) with varied values of constants (i.e., $C_u$ and $\alpha$), as well as calculation with linearand logarithmic velocity model (lin-log) (Eq. 14 and 15) as reference.

than both $C_{u\ VPE}$ with $\alpha$ = 1 as well as for $C_u$ = 4.5 with $\alpha$ = 1, except for C1, C2 and C3. It might be caused by large values of $C_{u\ VPE}$ for C1, C2 and C3 compared to other cases. From Figure 8, it seemed that none of the variation value of constants could provide a better fit estimation for whole depth (within and above interfacial sublayer), including the lin-log model, especially for C1, C2 and C3. In addition, based on velocities estimated by applying $C_u$ *fit* and $\alpha_{fit}$, HTF is capable to describe the profiles quite well near the bed. However, when depth is increasing, for example in B1 and B2 (H/ $\delta$ >3), the profiles seemed to deviate in the area above interfacial sublayer.

To observe the effects of each calculated value of the constants and to compare the HTF and lin-log models more clearly, the ratio between the averaged estimated (or calculated) and measured velocity ($\langle U\rangle_{calc}/\langle U\rangle_{meas}$) for the area within and above the interfacial sublayer, as well as the whole depth-averaged velocity, are presented through boxplots in Figure 10. Furthermore, the discrepancy ratio $A_r$, which is defined as $A_r$ (%) = [1-($\langle U\rangle_{calc}/\langle U\rangle_{meas}$)$_{\text{median}}$]100%, and the spread of the $\langle U\rangle_{calc}/\langle U\rangle_{meas}$ based on the interquartile range (IQR), defined as IQR = third quartile – first quartile from the boxplots in Figure 10, are also shown in Table 3 to evaluate each performance.

For the whole depth-averaged velocity (Figure 10a), $\langle U\rangle_{calc}/\langle U\rangle_{meas}$ was underestimated by variation values of $C_u$ and $\alpha$ (i.e., A, B, C and D) as well as by lin-log model (i.e., E). A showed an *Ar* relatively closer value to 1 compared to C. However, the spread (i.e., IQR) is comparatively larger. While B yielded better *Ar* and IQR values than A and C. Meanwhile, large variations were observed in the interfacial sublayer (Figure 10b) where A and B overestimated and underestimated the measurement, respectively. In contrast, C yielded the smallest difference from $\langle U\rangle_{meas}$ and smaller IQR values than A and E but similar to B. This implies that varied values of $\alpha$ have smaller effects on estimated velocities within the interfacial sublayer than the $C_u$ values.

For all averaged results (i.e., whole depth, interfacial sublayer and above the interfacial sublayer), the boxplots in Figure 10 are relatively right skewed judged from closer distance between median and first quartile. It implies that the variability of the estimated velocity profiles above the median was high, as can be seen in case C1, C2, and C3 (Figure. 9). Nevertheless, for C3, variability of estimated velocity profiles with variation values of $C_u$ and $\alpha$ as well as the lin-log model was lower than that in C1 and C2.

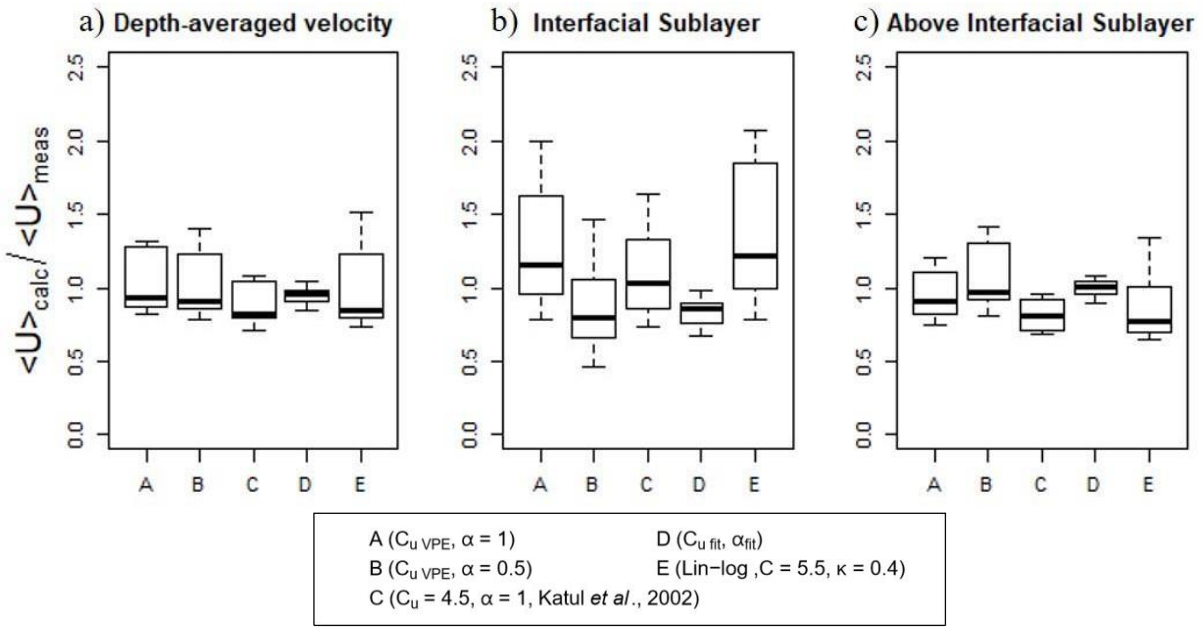


**Figure 10.** Comparisons of estimated velocity profiles with variation of constants values and velocity models (i.e., HTF and lin-log models) for all cases in data sets. From top to bottom, values in box plots correspond to the maximum, third quartile, median, first quartile, and minimum.


*Published by: Lembaga Penelitian dan Pengabdian Masyarakat (LPPM)*
*Institut Teknologi Sumatera, Lampung Selatan, Indonesia*

## Discussion

Figure 4 clearly shows that the changes in bed geometry (i.e. finer sediment addition onto gravel bed and different bed arrangement) affect the bed porosity and it can be seen from the roughness geometry function ($\varphi$ (z)). These changes also influenced the volume of fluid in the total area within the interfacial sublayer. Furthermore, overlapping particles (e.g., imbrication in C1, C2 and C3) obviously reduced the space for fluid significantly compared to a randomly packed bed (e.g., an armoured bed in A1-A3 and B1-B2).

Results from fitting Eq. 14 dan 15 with measured velocity profiles of data sets exhibited that constant $\alpha_{fit}$ increased as relative submergence increased in almost all cases. It implies that the changes in bed roughness seemed to have a linear relation with the ability of fluid to penetrate into the bed roughness. However, in A2 and A3, $\alpha_{fit}$ decreased with increasing relative submergence. This study argued that another factor may need to be considered. The two different types of finer sediments (i.e., gravel in C2 and C3 and sand in A2 and A3) possibly cause this condition. A study conducted by [35] showed that different mixtures of grain sizes (e.g., sand and pebbles versus coarse gravel and pebbles) can affect the porosity and permeability differently. The sand added in A2 and A3 might easily have clogged the voids available in the initial bed framework, which reduced the porosity and permeability to a greater extent than in C2 and C3. As porosity enhanced the penetration of turbulence [36], it reduced the $\alpha_{fit}$ in A2 and A3. This assumption is supported by the Reynolds stress profiles of each case, which are not shown here but are available in [31] and [23]. In study conducted by Nezu and Sanjou, it was found that the penetration of the Reynolds stress into the canopy becomes larger if the vegetation density decreases (i.e., becomes sparse) [37]. For A2 and A3, Reynolds stress was found to be unaffected by the sand addition. Meanwhile, the Reynolds stress penetrated and became more organized within the interfacial sublayer with the addition of gravels in C2 and C3 than in C1.

Regardless of the effects of different sizes of sediment mixtures, which is beyond our investigation here, the roughness geometry function showed a positive correlation with the changes in the velocity profiles within the interfacial sublayer as well as with $\alpha_{fit}$. An increase in the depth-averaged roughness geometry function (i.e., $\varphi_m$) triggers the fluid to penetrate deeper within the interfacial sublayer. This result is in good agreement with a study conducted by [37] that confirmed that denser vegetated canopies have a lower penetration depth than sparse canopies.

Furthermore, the present paper also examined the application of flow resistance VPE in order to determine the constant $C_u$ (Eq. 10) as one of the parameters needed in HTF. The differences of $C_u$ obtained from fitting with measurement data and those calculated using the VPE (Figure 8) imply that the values depend on the assumption whether mixing layer affected the whole depth velocity profile in the targeted study area. In other hands, If only the mixing layer is assumed to be exist (e.g, as in low relative submergence) the velocity profiles estimated by the HTF produce an almost constant value for $H/\delta \approx 1.5 - 2$ for $\alpha = 0.5$ and 1, respectively, as shown in Figure 2 and Figure 9. Thus, for relative submergence values higher than that (i.e., $H/\delta > 1.5 - 2$), a higher value of $C_{u\,fit}$ should be used to compensate this condition, especially for the area above the interfacial sublayer. Meanwhile, by applying the VPE to obtain flow resistance and inserting it to Eq. 10, as the flow resistance increased, the $C_{u\,VPE}$ decreased with an increase in the relative submergence.

From a study conducted by Raupach *et al* [25] over vegetation canopies, the averaged value of *Cu* was found to be 3.3, which is much smaller than the value of 5.8 calculated using the log law (i.e., Eq. 8. In this present study, based on Eq. 1, flow with a low relative submergence was assumed to have linear flow resistance near the stream bed [22]; thus, the calculated *Cu* must lie somewhere between 3.3 and 5.8. Although the same approach is implied from the value (i.e., *Cu* = 4.5) used by [16], our proposed method to calculate *Cu VPE* is based on consideration of the hydraulic conditions (e.g., relative submergence).

This proposed simple semi-empirical approach for estimating the two-dimensional double-averaged velocity profile assumes that only one type of mixing length (i.e., mixing layer) exists for relative submergence conditions of $H/\delta \leq 4$. In this range of relative submergence, in addition to the effect of bed roughness disturbing the existence of a logarithmic layer, this layer can also be potentially affected by the outer layer, as mentioned by [35]. Therefore, more than one type of mixing length may exist. This factor may explain the deviation in the velocity profiles at $z/\delta \approx 1.5 - 2$ (Figure 9). For example, because of the low relative submergence, the conditions in C1 and C2 were not only largely influenced by the bed roughness in the inner layer (i.e., near the bed area) but also for the outer layer (i.e., near the water surface), which reduced the velocity near the water surface. Unfortunately, measurement of velocity for C1, C2 and C3 was performed using Micro-ADV, which made measurement near the water surface relatively difficult.

## Conclusions

In the present paper, the condition in which the effect of bed roughness may extend to H/δ ≈ 4 and cause the nonexistence

of a logarithmic law layer was considered by assuming that the velocity profile may be dominantly governed by a mixing layer rather than the boundary layer. The applicability of the HTF was tested to describe the whole depth velocity profile. The way to determine the constants (i.e., Cu and $\alpha$) were slightly modified compared with the previous study by Katul *et al* [16].

A simple semi-empirical approach combining the flow resistance equation VPE and the mixing layer model HTF was tested to estimate the two-dimensional double-averaged velocity profile for flow with intermediate relative submergence (i.e., $2 \leq H/\delta \leq 4$) over artificial immobile gravel beds with various roughness densities and arrangements and with different bed conditions (i.e., sediment mixtures with the addition of finer sediment). A novel method to determine the constant parameter for the HTF using VPE (i.e., *Cu VPE*) was applied, and another constant value (i.e., $\alpha$) was evaluated based on the roughness geometry function. It is found that the roughness geometry function is an important parameter for understanding the behavior of flow within the interfacial sublayer.

This study suggest that the value of $\alpha = 1$ as used in [16] should not be generalized because it is affected by the bed geometry (e.g., bed arrangement, roughness geometry function, and porosity) and bed conditions (e.g., sediment mixtures) and may exert a dominant effect as the relative submergence decrease. Furthermore, even though depth-averaged velocities from velocity profiles calculated using *Cu VPE* with $\alpha = 0.5$ in the HTF underestimated the measurements, this approach still showed a better performance than the *Cu* values used in [14] for whole depth-averaged velocity and averaged velocity above interfacial sublayer (Figure 10) in these data sets. However, although the data set used in this study provide variation of bed geometry and bed conditions (e.g., sediment mixtures), the amount of data are limited. Additional tests may be required to strengthen these results.

Moreover, it is noticed that even though the HTF was suggested to be applicable for a wide range of relative submergence values (i.e., $0.2 < H/D < 7$), the existence of a complex mechanism that can be considered variation between two layers (i.e., within and above the interfacial sublayer) implies that more detailed investigations are needed to estimate the velocity profile rather than estimating the velocity from bulk flow conditions (i.e., *Ub*). In particular, for the studies that focus on the flow information in specific layers on micro-topographic scales, for example, investigation about flow characteristics within the roughness layer for habitat evaluation, for example is in [38].

## Conflicts of interest

There are no conflicts to declare.

## Acknowledgements

Experiments of [33] were conducted in Basin Hydrology Dynamics Laboratory, Gifu University, Japan.

## References

[1]. V. Nikora, K. Koll, I. McEwan, S. McLean and A. Dittrich, "Velocity Distribution in the Roughness Layer of Rough-Bed Flows", *Journal of Hydraulic Engineering*, vol. 130, no. 10, pp. 1036-1042, 2004.

[2]. D. Powell, "Flow resistance in gravel-bed rivers: Progress in research", *Earth-Science Reviews*, vol. 136, pp. 301-338, 2014.

[3]. T. Buffin-Bélanger, S. Rice, I. Reid and J. Lancaster, "Spatial heterogeneity of near-bed hydraulics above a patch of river gravel", *Water Resources Research*, vol. 42, no. 4, 2006.

[4]. M. Franca, R. Ferreira and U. Lemmin, "Parameterization of the logarithmic layer of double-averaged streamwise velocity profiles in gravel-bed river flows", *Advances in Water Resources*, vol. 31, no. 6, pp. 915-925, 2008.

[5]. S. Kara, T. Stoesser and T. Sturm, "Turbulence statistics in compound channels with deep and shallow overbank flows", *Journal of Hydraulic Research*, vol. 50, no. 5, pp. 482-493, 2012.

[6]. S. Mohajeri, S. Grizzi, M. Righetti, G. Romano and V. Nikora, "The structure of gravel-bed flow with intermediate submergence: A laboratory study", *Water Resources Research*, vol. 51, no. 11, pp. 9232-9255, 2015.

[7]. V. Nikora et al., "Double-Averaging Concept for Rough-Bed Open-Channel and Overland Flows: Applications", *Journal of Hydraulic Engineering*, vol. 133, no. 8, pp. 884-895, 2007.

[8]. Luchini, "Universality of the Turbulent Velocity Profile", *Physical Review Letters*, vol. 118, no. 22, 2017.

[9]. J. Bathurst, D. Simons and R. Li, "Resistance Equation for Large-Scale Roughness", *Journal of the Hydraulics Division*, vol. 107, no. 12, pp. 1593-1613, 1981.

[10]. M. Rouzes, F. Moulin, E. Florens and O. Eiff, "Low relative-submergence effects in a rough-bed open-channel flow", *Journal of Hydraulic Research*, vol. 57, no. 2, pp. 139-166, 2018.

[11]. V. Nikora, D. Goring, I. McEwan and G. Griffiths, "Spatially Averaged Open-Channel Flow over Rough Bed", *Journal of Hydraulic Engineering*, vol. 127, no. 2, pp. 123-133, 2001.

[12]. R. Gaudio, A. Miglio and S. Dey, "Non-universality of von Kármán's κ in fluvial streams", *Journal of Hydraulic Research*, vol. 48, no. 5, pp. 658-663, 2010.

[13]. K. Koll, "Parameterisation of the vertical velocity profile in the wall


*Published by: Lembaga Penelitian dan Pengabdian Masyarakat (LPPM)*
*Institut Teknologi Sumatera, Lampung Selatan, Indonesia*

region over rough surfaces", in *Proceedings of the International Conference on Fluvial Hydraulics, River Flow 2006*, pp. 163-171, 2006.

[14]. X. Chen, M. Hassan, C. An and X. Fu, "Rough Correlations: Meta-Analysis of Roughness Measures in Gravel Bed Rivers", *Water Resources Research*, vol. 56, no. 8, 2020.

[15]. V. Nikora, K. Koll, S. McLean, A. Dittrich, and J. Aberle, "Zero-plane displacement for rough-bed open-channel flows", *Proceeding of International Conference Fluvial Hydraulics*, Louvain-la-Neuve, Belgium, vol. 1, pp. 83–92, 2002b.

[16]. G. Katul, P. Wiberg, J. Albertson and G. Hornberger, "A mixing layer theory for flow resistance in shallow streams", *Water Resources Research*, vol. 38, no. 11, pp. 32-1-32-8, 2002.

[17]. S. Dey and R. Das, "Gravel-Bed Hydrodynamics: Double-Averaging Approach", *Journal of Hydraulic Engineering*, vol. 138, no. 8, pp. 707-725, 2012.

[18]. V. Ferro and P. Porto, "Assessing theoretical flow velocity profile and resistance in gravel bed rivers by field measurements", *Journal of Agricultural Engineering*, vol. 49, no. 4, pp. 220-227, 2018.

[19]. A. Adak, "Turbulent Flow Characterization over the Gravel Bed", *IOP Conference Series: Materials Science and Engineering*, vol. 377, p. 012090, 2018.

[20]. M. Luo, X. Wang, X. Yan and E. Huang, "Applying the mixing layer analogy for flow resistance evaluation in gravel-bed streams", *Journal of Hydrology*, vol. 589, p. 125119, 2020.

[21]. M. Lamb, F. Brun and B. Fuller, "Hydrodynamics of steep streams with planar coarse-grained beds: Turbulence, flow resistance, and implications for sediment transport", *Water Resources Research*, vol. 53, no. 3, pp. 2240-2263, 2017.

[22]. R. Ferguson, "Flow resistance equations for gravel- and boulder-bed streams", *Water Resources Research*, vol. 43, no. 5, 2007.

[23]. D. Rickenmann and A. Recking, "Evaluation of flow resistance in gravel-bed rivers through a large field data set", *Water Resources Research*, vol. 47, no. 7, 2011.

[24]. A. Michalke, "On the inviscid instability of the hyperbolictangent velocity profile", *Journal of Fluid Mechanics*, vol. 19, no. 4, pp. 543-556, 1964.

[25]. M. Raupach, J. Finnigan and Y. Brunei, "Coherent eddies and turbulence in vegetation canopies: The mixing-layer analogy", *Boundary-Layer Meteorology*, vol. 78, no. 3-4, pp. 351-382, 1996.

[26]. G. Katul, "An Investigation of Higher-Order Closure Models for a Forested Canopy", *Boundary-Layer Meteorology*, vol. 89, no. 1, pp. 47-74, 1998.

[27]. H. Jobson, "Evaporation Into the Atmosphere: Theory, History, and Applications", *Eos, Transactions American Geophysical Union*, vol. 63, no. 51, p. 1223, 1982.

[28]. P. Wiberg and J. Smith, "Velocity distribution and bed roughness in high-gradient streams", *Water Resources Research*, vol. 27, no. 5, pp. 825-838, 1991.

[29]. D. Poggi, A. Porporato, L. Ridolfi, J. Albertson and G. Katul, "The Effect of Vegetation Density on Canopy Sub-Layer Turbulence", *Boundary-Layer Meteorology*, vol. 111, no. 3, pp. 565-587, 2004.

[30]. D. Pokrajac, J. J. Finnigan, C. Manes, I. Mcewan, and V. Nikora, "On the definition of the shear velocity in rough bed open channel flows", *River Flow 2006*, 2006.

[31]. L. Ferreira, "Impact of Sediment Overfeeding in Gravel-Bedded River's Salmonid Habitats", (MSc thesis), Instituto Superior Técnico, TU Lisbon, 2008.

[32]. S. Habib, N. Tanaka and Y. Yoshizawa, "Open Channel Turbulence Characteristics in a Roughness Layer for Small Water Depth Relative to Roughness Elements Height", *Journal of Japan Society of Civil Engineers, Ser. B1 (Hydraulic Engineering)*, vol. 72, no. 4, pp. I_511-I_516, 2016.

[33]. R. Yanda, M. Harada and I. Tamagawa, "The Effects of Sediment Supply on Hydraulic Characteristics of Flow Over The Imbricated Cobbles", *Journal of Japan Society of Civil Engineers, Ser. B1 (Hydraulic Engineering)*, vol. 72, no. 4, pp. I_613-I_618, 2016.

[34]. W. F. COON, "Estimation of Roughness Coefficients for Natural Stream Channels with Vegetated Banks", *Pubs.usgs.gov*, 2022.

[35]. P. Kamann, R. Ritzi, D. Dominic and C. Conrad, "Porosity and Permeability in Sediment Mixtures", *Ground Water*, vol. 45, no. 4, pp. 429-438, 2007.

[36]. H. Chan, W. Huang, J. Leu and C. Lai, "Macroscopic modeling of turbulent flow over a porous medium", *International Journal of Heat and Fluid Flow*, vol. 28, no. 5, pp. 1157-1166, 2007.

[37]. I. Nezu and M. Sanjou, "Turburence structure and coherent motion in vegetated canopy open-channel flows", *Journal of Hydro-environment Research*, vol. 2, no. 2, pp. 62-90, 2008.

[38]. M. Harada, R. Yanda, O. Yukio, K. Yuichi, "Swimming fish habitat evaluation concept focusing on flow characteristics around the roughness layer in streams", in *Proceedings of the 37th IAHR World Congress*, Kuala Lumpur, Malaysia, pp. 1-6, 2017